

The physics of GRB jets and their interaction with the progenitor star

DAVIDE LAZZATI⁽¹⁾, BRIAN J. MORSONY⁽¹⁾, and MITCHELL C. BEGELMAN⁽¹⁾

⁽¹⁾ *JILA, University of Colorado, 440 UCB, Boulder, CO 80309-0440*

Summary. — It is now generally accepted that long gamma-ray bursts are associated with the final evolutionary stages of massive stars. As a consequence, their jets must propagate through the stellar progenitor and break out on their surface, before they can reach the photospheric radius and produce the gamma-ray photons. We investigate the role of the progenitor star in shaping the jet properties. We show that even a jet powered by a steady engine can develop a rich phenomenology at the stellar surface. We present special-relativistic simulations and compare the results to analytic considerations. We show that the jet is complex in the time as well as in the angular domain, so that observers located along different lines of sight detect significantly different bursts.

PACS 98.76.Rz - 98.38.j - 95.30.Dr - .

1. – Introduction

Long duration gamma-ray bursts (GRBs) are likely produced by the dissipation of bulk kinetic energy in a relativistic flow with a Lorentz factor of at least 100. The presence of supernova features in the afterglow of several events[2] implies that the outflow has to propagate through a stripped massive star at the end of its evolution before producing the gamma-rays we observe. There are therefore three mechanisms playing a role in shaping the GRB light curves: the inner engine, the hydrodynamic interaction with the progenitor star and the dissipation/radiative mechanism. Which of these is the dominant one is poorly understood.

We present high resolution numerical simulations of relativistic jets propagating through the core of massive stars[1]. The simulations, performed with the adaptive mesh refinement (AMR) special relativistic hydro code FLASH, are tailored to shed light on the second question above: what properties in the outflow are imprinted by its propagation through the star. To this aim, we inject a flow with constant properties in the center of the star, we propagate it, and we study the phenomenology on the jet emerging on the stellar surface.

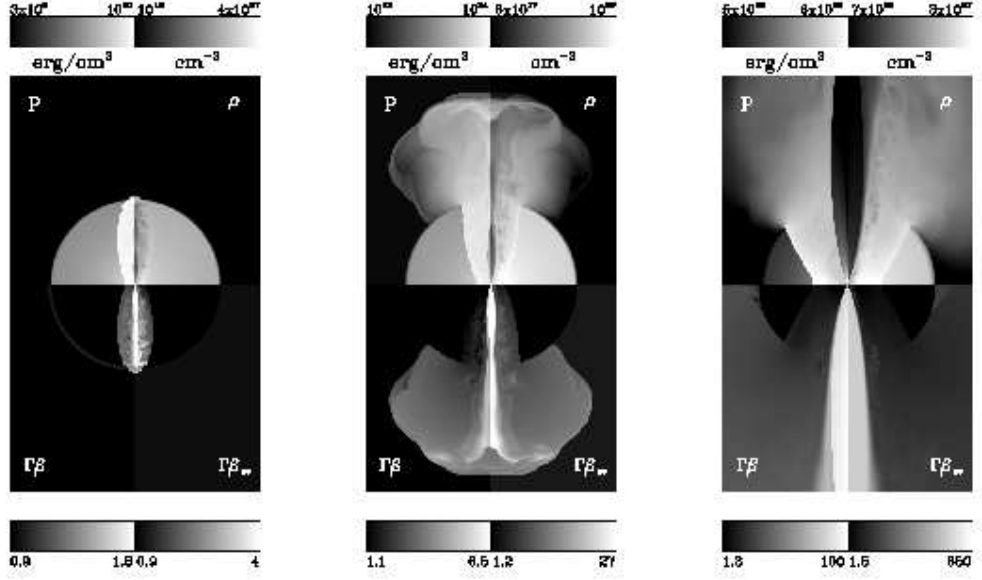


Fig. 1. – Stills from a simulation of a relativistic jet with $\theta_0 = 10^\circ$, $L = 2.66 \times 10^{50} \text{ erg s}^{-1}$, and $\Gamma_0 = 5$. The jet propagates through a star with $R = 10^{11} \text{ cm}$, a power-law density profile and a mass of $M = 15M_\odot$. Each of the three panels is divided into four sub-panels, each showing a different quantity. Starting from the upper right panel, in clockwise order, panels show the density, the Lorentz factor achievable at infinity, the actual Lorentz factor and the pressure. The gray-scale is always logarithmic. The first panel shows a still at 10.3 seconds after the moment at which the engine is turned on. The middle panel shows a still at 15 seconds, while the right panel shows a still at 40 seconds. The jet is in the shocked phase in the central panel and in the un-shocked phase in the right panel.

2. – Phases

The development of the relativistic flow is shown in the simulations to proceed through four subsequent phases, three of which are radiative and can, potentially, be observed in the GRB light curves. Initially (see also the left panel of Fig. 1), the jet is bounded inside the star. Its head propagates subrelativistically, yet highly supersonically, creating a bow shock that recycles shocked hot jet material in a cocoon that surrounds the jet itself. The cocoon pressure recollimates the jet, that propagates through the star with an opening angle much smaller than the one with which it was injected (10 degrees in our simulations).

With a propagation speed of several tens of per cent the speed of light, the head of the jet reaches the surface of the star 5 to 10 seconds after the jet is initiated (left panel of Fig. 1). At this point, the cocoon energy is released[3]. The cocoon is made of hot jet material, partially mixed through vortex shedding with the stellar material. It does not have relativistic bulk motion, but has a potential adiabatic acceleration up to Lorentz factors of several tens. Since it is released through a nozzle on the stellar surface it is almost isotropic.

Simultaneously to the release of the cocoon, the relativistic jet emerges out of the star and propagates. It has already achieved large, albeit unsteady, values of Lorentz

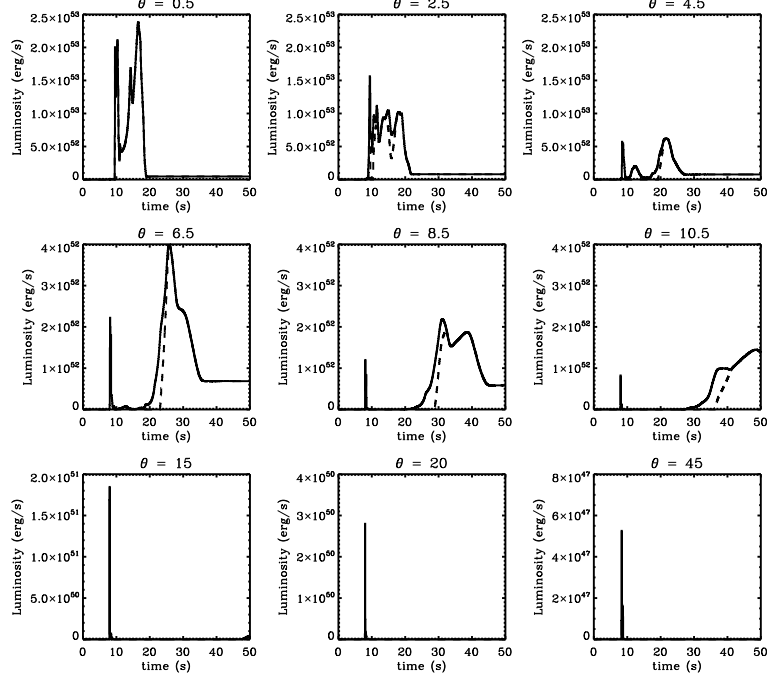


Fig. 2. – Light curves of the kinetic luminosity emerging out of the stellar surface for observers located at different angles with respect to the jet axis. Solid lines show the kinetic luminosity of all the material with $\Gamma_\infty \geq 2$, where Γ_∞ is the maximum achievable Lorentz factor in an adiabatic expansion. For comparison, dashed lines show the luminosity of the material with $\Gamma_\infty \geq 100$. The data are from simulation 16Tig5[1] that has $\theta_0 = 10^\circ$ and $\Gamma_0 = 5$. The flattening of the light curves at late times (especially evident in the $\theta = 6.5^\circ$ and $\theta = 8.5^\circ$ cases) is due to the unshocked phase, when the jet enters a steady state.

factor, and so it stays collimated. In this phase, that we call the shocked jet phase, the jet properties are severely affected by the struggle to propagate through a cold and dense stellar core (central panel of Fig. 1). The jet material has been repeatedly shocked and is characterized by alternated high-density/low- Γ and low-density/high- Γ regions and by the presence of lateral shocks. The opening angle fluctuates in this phases, but does not have a regular increase or decrease, always being limited to several degrees. This phase lasts few tens of seconds, depending on the stellar properties.

Eventually, as the cocoon pressure wanes, the jet settles into a more stable condition, in which the core of the jet expands freely until impacts a shear layer that separates it from the stellar material (right panel of Fig. 1). The free-jet/shear layer are separated by a strong shock. In this phase the jet opening angle widens[4], until the limiting opening angle $\theta_{\text{lim}} = \theta_0 + \Gamma_0^{-1}$ is reached, where the right hand quantities are the injection values of opening angle and Lorentz factor. Very small temporal variability is given to the flow by the propagation through the star in this phase. It is therefore possible that variability at late stages, if detected, would give us insight in the properties of the inner engine.

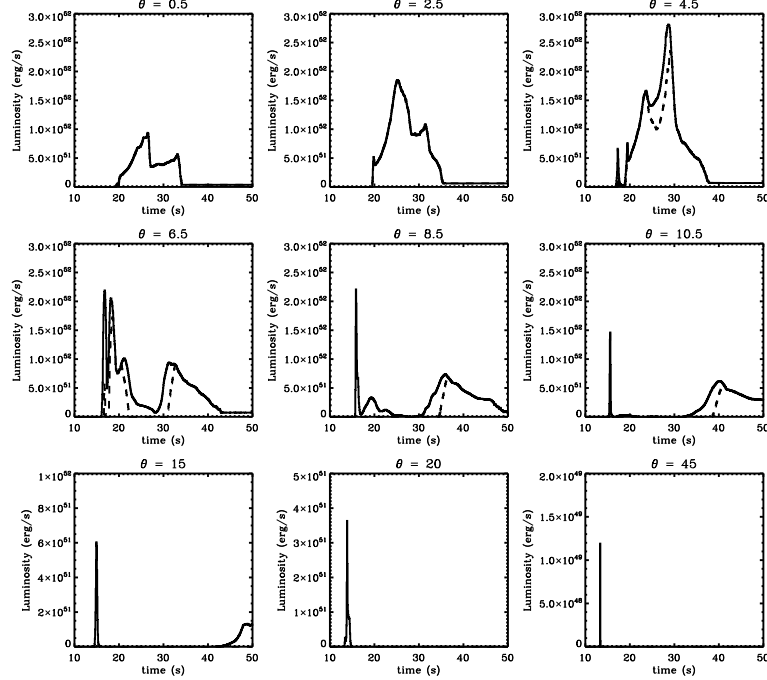


Fig. 3. – Same as Fig. 2 but for data from the simulation 16Tig2, that has a lower initial Lorentz factor $\Gamma_0 = 2$.

3. – Light curves

Due to the complex evolution of the jet propagation inside and outside of the star, different observers will detect different bursts. In this section we discuss the light curves obtained for different observers as a function of the off-axis angle. Since neither the dissipation mechanism nor the radiative process that produce the final GRB light curves are known, we discuss here the kinetic luminosity of the outflow. In addition we compute our light curves just outside the stellar surface, even though the interaction between different parts of the flow is not over yet and can lead to some modifications at the radiative radius. Light curves for different viewing angles and initial conditions are shown in Fig. 2 and 3. In each figure we show the light curve of highly relativistic material ($\Gamma \geq 100$), capable of producing γ -rays, and of material that is at least mildly relativistic ($\Gamma \geq 2$), more relevant to X-ray and afterglow components.

3.1. The large-angle observer. – Consider an observer located far from the jet axis, at an angle $\theta > \theta_0 + \Gamma_0^{-1}$. Due to the above considerations the jet will never expand wide enough so that the observer could see it directly. The cocoon release results however in a much wider outflow and cocoon emission would be detected along large-angle lines of sight. Due to its wide angle and limited energetics, cocoon emission is rather weak, as can be seen in the bottom line of Fig. 2 and 3. Events observed under such conditions could be GRB 980425 and/or GRB031203. The lack of detection in the radio band of off-axis jet emission is however difficult to account for, at least in the first case[5].

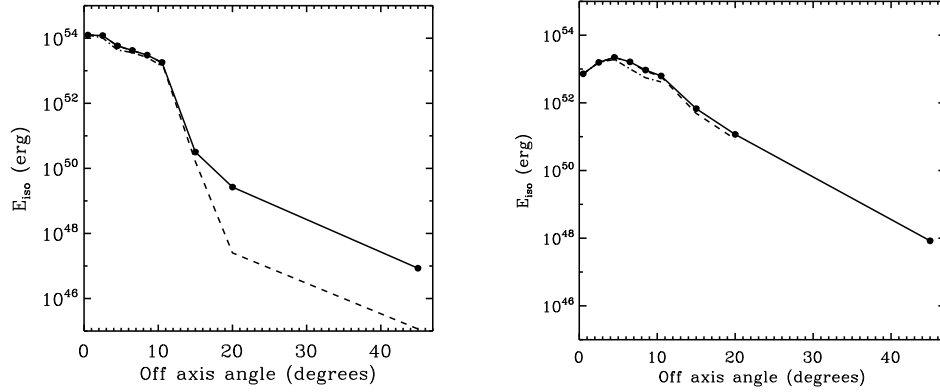


Fig. 4. – Isotropic equivalent energy versus off-axis angle for the light curves in Fig. 2 and 3. The solid line shows all the energy of material with $\Gamma_0 \geq 2$ while the dashed line shows only the energy of material with $\Gamma_0 \geq 100$.

3.2. The intermediate observer. – Consider now an intermediate observer. Its viewing angle is located outside the jet opening angle during the shocked jet phase, but inside the limiting opening angle of the un-shocked phase. This observer will initially detect the cocoon emission, that will be identified as a weak precursor[6]. During the shocked jet phase, the outflow is beamed inside a small opening angle and our observer does not detect any emission. Eventually, as the jet opening angle spreads to include the line of sight, the main GRB emission is detected. Initially, the emission is due to the bright shear layer. Eventually, the un-shocked jet emission is seen, characterized by a steady, weak luminosity. It is during this phase, probably elusive and hard to detect, that the inner engine is seen “directly”.

3.3. The on-axis observer. – Consider finally an observer located within the opening angle of the shocked jet phase. This observer will detect radiation at all stages. Initially she/he will detect the cocoon energy, followed, without any interruption or dead time, by the shocked jet emission. This is the brightest phase, since all the jet energy is concentrated in the small opening angle of the shocked jet (see the top panels of Fig. 2 and 3). Strong variability, especially in the highly relativistic component ($\Gamma \geq 100$, dashed line in the figures), is present in this phase, due to the jet-cocoon interaction. After the shocked jet phase, the light curve sharply transitions to the unshocked jet.

The comparison of the various panels of Fig. 2 and 3 shows that the brightest light curves are observed close to the symmetry axis. Fig. 4 shows the total isotropic equivalent energy versus the off-axis angle. As underlined by the linear-logarithmic scale, the jet profile is well described by an exponential drop, especially if all the relativistic material is considered. A very sharp jet/no-jet transition is instead observed if only the hyper-relativistic material is singled out ($\Gamma_\infty \geq 100$).

4. – Summary

We have presented AMR special relativistic hydro simulations of a relativistic light jet propagating through the core of a massive star. We concentrate on the interaction of the

jet with the stellar material, showing that the emerging jet displays a rich phenomenology of temporal and angular properties. We compute light curves and show that they present some features observed in observations. In particular, quasi isotropic cocoon outflow and the widening of the jet opening angle can explain long dead times and precursors as observed in BATSE and Swift light curves.

* * *

The software used in this work was in part developed by the DOE-supported ASC/Alliance Center for Astrophysical Thermonuclear Flashes at the University of Chicago. This work was supported by NSF grant AST-0307502, NASA Astrophysical Theory Grant NNG06GI06G, and Swift Guest Investigator Program NNX06AB69G. This work was partially supported by the National Center for Supercomputing Applications under grant number AST050038 and utilized the NCSA Xeon cluster.

REFERENCES

- [1] MORSONY B. J., LAZZATI D. and BEGELMAN M. C., *ApJ submitted (astro-ph/0609254)*, (2006)
- [2] STANEK, K. ET AL., *ApJ*, **591** (2003) L17
- [3] RAMIREZ-RUIZ E., CELOTTI A. and REES M. J., *MNRAS*, **337** (2002) 1349
- [4] LAZZATI D. and BEGELMAN M. C., *ApJ*, **629** (2005) 903
- [5] WAXMAN E., *ApJ*, **605** (2004) L97
- [6] LAZZATI D., *MNRAS*, **357** (2005) 722